Reconstructing magma failure and the degassing network of dome-building eruptions

Yan Lavallée[1,2], Philip M. Benson[3], Michael J. Heap[4], Kai-Uwe Hess[2], Asher Flaws[2], Burkhard Schillinger[5], Philip G. Meredith[6], and Donald B. Dingwell[2]

[1]Earth, Ocean and Ecological Sciences, University of Liverpool, Liverpool L69 3GP, UK
[2]Earth and Environmental Sciences, University of Munich, 80333 Munich, Germany
[3]Earth and Environmental Sciences, University of Portsmouth, Portsmouth, Hampshire PO1 2UP, UK
[4]École et Observatoire des Sciences de la Terre, Université de Strasbourg (UMR 7516 Centre National de la Recherche Scientifique), F-67081 Strasbourg Cedex, France
[5]Forschungsreaktor FRM-II, Technische Universität München, 85747 Garching, Germany
[6]Department of Earth Sciences, University College London, London WC1E 6BT, UK

ABSTRACT

Volcanic eruptions are regulated by the rheology of magmas and their ability to degas. Both detail the evolution of stresses within ascending subvolcanic magma. But as magma is forced through the ductile-brittle transition, new pathways emerge as cracks nucleate, propagate, and coalesce, constructing a permeable network. Current analyses of magma dynamics center on models of the glass transition, neglecting important aspects such as incremental strain accommodation and (the key monitoring tool of) seismicity. Here, in a combined-methods study, we report the first high-resolution (20 μm) neutron-computed tomography and microseismic monitoring of magma failure under controlled experimental conditions. The data reconstruction reveals that a competition between extensional and shear fracturing modes controls the total magnitude of strain-to-failure and importantly, the geometry and efficiency of the permeable fracture network that regulates degassing events. Extrapolation of our findings yields magma ascent via strain localization along conduit margins, thereby providing an explanation for gas-and-ash explosions along arcuate fractures at active lava domes. We conclude that a coupled deformation-seismicity analysis holds a derivation of fracture mechanisms and network, and thus holds potential application in forecasting technologies.

INTRODUCTION

In volcanic systems, the rheology of magmas is of paramount importance. During pre- or syneruptive ascent, magmas undergo decompression resulting in crystallization, temperature change, volatile exsolution, and degassing (Martel and Schmidt, 2003). Any magmatic gas trapped in the porous network will exert stress against the condensed phases of the magma (melt and crystals), whose resultant deformation is distributed in time via melt rheology. These processes typically result in a nonlinearly depth-dependent magma viscosity, which in turn induces nonlinear ascent dynamics and strain rate variation within the magma column. Such rheological changes are ultimately manifested in eruption style, with competition between the characteristic times imposed by the strain rates and the material stress relaxation times posing the volcanic dilemma: "flow or blow" (Dingwell, 1996).

Dome-building eruptions, with their cycles of endogenous and exogenous growth, commonly followed by destruction, epitomize a switch in magma rheology (Hale and Wadge, 2008). Endogenous growth proceeds as long as pervasive viscous and/or plastic deformation mechanisms dominate, but upon strain localization and shear rupture, growth may proceed exogenously (Watts et al., 2002), generating distinct nondestructive, low-frequency, seismic signals (Neuberg et al., 2006) and may, upon further seismic slip, erect spine-like structures (Kendrick et al., 2012). The buildup of internal gas pressure is a threat to the structural stability of lava domes. Failure of lava domes frequently generates Vulcanian eruptions (Lavallée et al., 2012); in extreme cases, dome collapse may lead to severe decompression, triggering catastrophic explosive eruptions (Spieler et al., 2003). The depressurization path of magma during ascent is controlled by the development of permeability via a network of bubbles (Wright and Weinberg, 2009) and microfractures (Mueller et al., 2005), leading to degassing events with contrasting patterns and recurrences (Varley and Taran, 2003). At Santiaguito volcano (Guatemala), for example, the active dome displays spectacular, hourly gas-and-ash explosions along concentric ring fractures (Johnson et al., 2008), posing tempting questions regarding the geometry of the underlying permeable, degassing network and its relationship to strain localization in magma (e.g., Jellinek and Bercovici, 2011). Numerical models of magma ascent have tested the role of conduit geometry changes (as illustrated by petrographical and field studies; Noguchi et al., 2008) and demonstrated their importance in reducing the confining stress acting on ascending magma and in the creation of both shear and extensional faults (Thomas and Neuberg, 2012). Structural studies of domes partially dissected by explosive eruption provide evidence for the development of these fault types in the roots of domes, which expose pervasive and/or localized permeable networks of faults (Watts et al., 2002).

The fragmentation of magma occurs at the ductile-brittle or "glass" transition (Dingwell, 1996). Although fragmentation is common to all explosive eruptions, the path to fragmentation undoubtedly varies considerably with eruption type. The first analysis of magma failure at the glass transition consisted of the application of a Maxwell body analysis to the viscoelasticity of silicate liquids. In this analysis, the conditions of failure are, for a given liquid chemistry, constrained by temperature and strain rate (Dingwell, 1996). Silicate liquids are Newtonian fluids at low to moderate strain rates, but at the extremely high strain rates anticipated in explosive eruptions, the viscosity becomes non-Newtonian and the liquids will, under conditions of sustained stress, fail in a brittle manner, generating as they do seismicity (Tuffen et al., 2008). This situation is further complicated by the fact that the magmas involved in such eruptions contain crystals; the amount may vary remarkably but their presence is ubiquitous. In conditions that yield Newtonian melt viscosity for pure liquids, crystal-bearing magmatic suspensions may adopt a non-Newtonian, shear-thinning rheology (Lavallée et al., 2007). The presence of crystals also impacts the coefficients of brittle response, with failure typically setting in at strain rates two to three orders of magnitude lower than in the crystal-free case (Gottsmann et al., 2009). However, the current lack of any failure criterion (e.g., Mohr-Coulomb) for magma inhibits failure analyses based on the stress tensor. Recent experimental observations demonstrate that deformation leading to failure is accompanied by a supraexponential increase in microseismicity, measured as acoustic emissions (AE) (Lavallée et al., 2008). Bearing in mind that seismic signals constitute a key indicator of volcanic unrest (Papale, 1999; Scarpa, 2001), and that such information thus has broad impact in hazard mitigation scenarios, our investigation of magma failure and its associated permeable network incorporated in situ AE monitoring. This ensemble of (1) experimental deformation, (2) real-time AE monitoring, (3) ultrasonic testing,

GEOLOGY, April 2013; v. 41; no. 4; p. 515–518; Data Repository item 2013143 | doi:10.1130/G33948.1 | Published online 20 February 2013

and importantly (4) recent developments in high-resolution (20 μm) neutron-computed tomography (NCT) imaging places the mechanistic understanding of magma failure and creation of permeable fracture networks in lava domes on a new basis.

MATERIALS AND METHODS

The failure of dome lavas across the ductile-brittle transition (i.e., the nondiscrete transition between deformation behavior considered macroscopically ductile and that considered macroscopically brittle; Rutter, 1986) was investigated by varying the uniaxial stress imposed on dome lava from Volcán de Colima (with 50%–60% crystals and 7% pores) at an eruptive temperature of 940 °C (Lavallée et al., 2012) (see the GSA Data Repository[1] for details of the methods and analyses). Following previous observations of the onset of cracking in such lavas (at axial stresses ≥20 MPa), experiments were performed at constant stresses of 20, 28.5, 46, and 76 MPa to assess the total strain-to-failure and monitor the precursory AE activity. The amplitude distribution of recorded AE events was subjected to a statistical analysis analogous to the Gutenberg-Richter seismic *b*-value (i.e., gradient of frequency of occurrence to magnitude) to assess the relative importance of fracture scaling and localization. The AE data were then subjected to a failure forecast model (Voight, 1988) to test its accuracy across the ductile-brittle transition. For samples in which deformation was arrested immediately prior to complete failure, we probed the degree of fracturing via porosity and ultrasonic measurements, and reconstructed the permeable fracture network via NCT.

DEFORMATION RESULTS AND REGIMES OF MAGMA

At an applied stress of 20 MPa, magma deformation was macroscopically ductile (i.e., the sample did not succumb to failure within the imposed 35% strain limit); yet bulging induced the growth of a pervasive network of fractures near the sample edge. In contrast, deformation at higher stresses of 28.5, 46, and 76 MPa showed an increasingly brittle response manifested by lower total strain-to-failure and lower AE *b*-values (Table 1), indicating a shift from small-scale distributed cracking (i.e., ductile) to large-scale, more localized cracking (i.e., brittle) (Main et al., 1989). The buildup to failure under compressive stress encompassed the nucleation of tensile fractures, which progressively propagated and coalesced, simultaneously releasing AE at an accelerating rate. Application of the failure forecast method to the recorded AE energy provided equally accurate forecasts, irrespective of the applied stress and thus total strain (or more importantly, time available) to achieve failure. This remained true whether we used the complete AE data set or only the first 50% of recorded AE data. Our initial experimental analyses are therefore generally consistent with field observations, reflecting how transient stress– (and strain rate–) dependent rheologies are driven by the interplay between ductile and brittle components, yielding significant changes in microstructures and, hence, a seismicity-generating mechanism (Main et al., 1989).

Deformation in the brittle regime significantly changes the physical properties of the magma. Optical microscopic analysis revealed an evolution from crystal reorientation and alignment to crystal dislocation and fracturing across the ductile-brittle transition. Specifically, deformation across this transition produced substantial increases in porosity associated with the development of a dilatant fracture network (Table 1). This dilatancy also resulted in significant reductions in ultrasonic P-wave and S-wave velocities of up to 40% and 35%, respectively.

TABLE 1. CHARACTERISTICS OF MAGMA FAILURE WITH APPLIED STRESS

	28.5 MPa	46 MPa	76 MPa
Total strain-to-failure (%)	18.0	12.0	5.5
AE *b*-value*	3.6	2.7	2.4
Porosity increase by fractures (%)	14.1	10.9	20.9

*AE—acoustic emissions; *b*-value—Gutenberg-Richter seismic *b*-value.

IMAGING THE PERMEABLE FRACTURE NETWORK

The fracture networks developed by the deformation of magma have been imaged via NCT (Fig. 1; tomography Movie DR1A and Movie DR1B are available in the Data Repository). In our analysis, each identified fracture was assigned a location, and the density of fractures was collapsed onto the sample half-space. The geometry of the fracture network was then correlated with the magnitude of the applied stress. Two primary modes of deformation can be recognized over the stress conditions investigated. For deformation at the onset of the ductile-brittle transition (i.e., at an applied stress of 28.5 MPa), we observe a disintegration of the sample through distributed micro- and mesoscopic fractures (Fig. 1A), with axial fractures restricted to within the barreled section. Crosscutting relationships show that axial, extensional microfractures first propagated, and were subsequently crosscut by shear fractures at an angle of ~45° from the principal compressive stress (Fig. 1A). The axial fractures are wider than the shear fractures, thus dominating the development of the porous network. Conversely, for deformation at the brittle end of the ductile-brittle transition (i.e., 76 MPa), the fault structure is characterized by a more

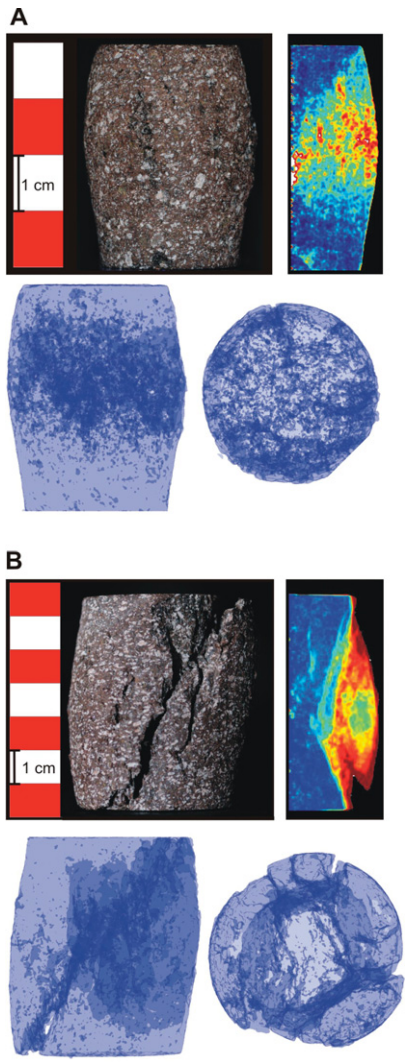

Figure 1. Fracture networks induced by magma failure. The photograph of each sample is accompanied by the neutron-computed tomography (NCT) reconstructions of the fracture network (below) and the modeled density of fractures (color-coded, where red is heavily fractured and blue is intact) represented in a half-space (right). A: Sample deformed at 28.5 MPa shows a pervasive distribution of tensional fractures with predominance in the barreled area. Shear fractures focus along an hourglass shape at an angle of ~45° from the principal compressive stress. B: Sample deformed at 76 MPa developed strongly localized shear fractures along an hourglass geometry at an angle of ~20° from the principal compressive stress.

[1]GSA Data Repository item 2013143, sample, methods, and analyses, is available online at www.geosociety.org/pubs/ft2013.htm, or on request from editing@geosociety.org or Documents Secretary, GSA, P.O. Box 9140, Boulder, CO 80301, USA.

localized distribution of macroscopic shear fractures with minor extensional cracks being restricted to the central region of the sample (Fig. 1B). The shear fractures formed a large hourglass shape at an angle of ~20° from the applied compressive stress. In this scenario, the macroscopic shear fractures were responsible for the volume increase and the development of a porous network. NCT reveals that nucleation and propagation of fractures is distributed at low applied stresses (and strain rates) whereas failure at high values of applied stresses (and resultant strain rates) develops via strongly localized shear planes.

As noted earlier, the key control on degassing at active lava domes lies in the ability of fracture coalescence to create a permeable network. Using the tomographic reconstruction of the permeable fracture network, we assess the permeability (κ) of the experimentally developed shear zones (e.g., Bai et al., 2011; Pan et al., 2010) via the porosity (ϕ) following the relationship (Mueller et al., 2005):

$$\kappa = 10^{-17}\phi^{3.4}. \quad (1)$$

This relationship combined with the porous damage induced by shear imaged by NCT provides a first-order map of the permeability development during magma failure (Fig. 2). Although the total porosity increases via fracturing were comparable and led to similar bulk permeability increases, analysis of the directional crack density from the NCT highlighted contrasting anisotropy of the fracture networks in the different experiments. Application of the relationship in Equation 1 to the imaged crack density illustrates the anisotropy of the permeable fracture network (Fig. 2), showing an extreme anisotropy parallel to the direction of applied stress (i.e., axial) in the sample deformed at 76 MPa, compared to the orthogonal (i.e., lateral) anisotropy of the sample deformed at 28.5 MPa. These distinct constructional scenarios carry important consequences to the ability of magma to degas in upper volcanic conduits and ultimately, achieve fragmentation.

AN "ARCHITECTURE" OF MAGMATIC FRAGMENTATION

A reliable forecast of the timing and style of volcanic activity is beyond current methods. Such an approach ultimately requires a thorough understanding of the stress conditions experienced by magma during ascent as well as the mechanics of magma failure, the architecture of the permeable network, and its seismic character. The data presented here illustrate some of these relationships. NCT revealed that the stress exerted on the magma controls the style of fractures, expressed in the microseismic record via the *b*-value. Even under compression, fracturing nearly always initiates by the generation of tensile cracks, which coalesce to form shear fractures (e.g., Rutter, 1986)—a mechanism especially important to magma ascent and failure in conduits. This fracture style, in turn, controls the development of the fracture network, including the time available to achieve (and thus to forecast) failure. It follows that fragmentation processes proceeding via different ratios of extensional/shear fractures are potentially responsible for the wide range of eruptive styles currently observed at active lava domes. During dome-building eruptions, the flow of non-Newtonian, crystal-bearing magma is not Hagen-Poiseuille, but that of a plug. Rheologically, the shear-thinning nature of magma favors the localization of strain (and stress) along the conduit margins (Thomas and Neuberg, 2012) as demonstrated by the formation of shear bands in magma near conduit margins and fracture-controlled exogenous growth (Hale and Wadge, 2008). It follows from our experimental analysis that such a strain distribution undoubtedly results in an anisotropic permeable fracture network with variable degassing efficiency (Laumonier et al., 2011), which may in turn reduce the potential for large explosive eruptions (Mueller et al., 2005). Our experiments reveal that magma deformation at the ductile end of the ductile-brittle transition produces a monotonically increasing density of tensile microfractures that results in a large volumetric expansion and a pervasive (yet mildly anisotropic) fracture network. At the brittle end of the ductile-brittle transition, deformation proceeds faster and fracturing is more localized, highly anisotropic, and subparallel to the principal shear direction (Fig. 3A). Such contrasting anisotropy of the permeability distribution is likely to strongly influence the pathways

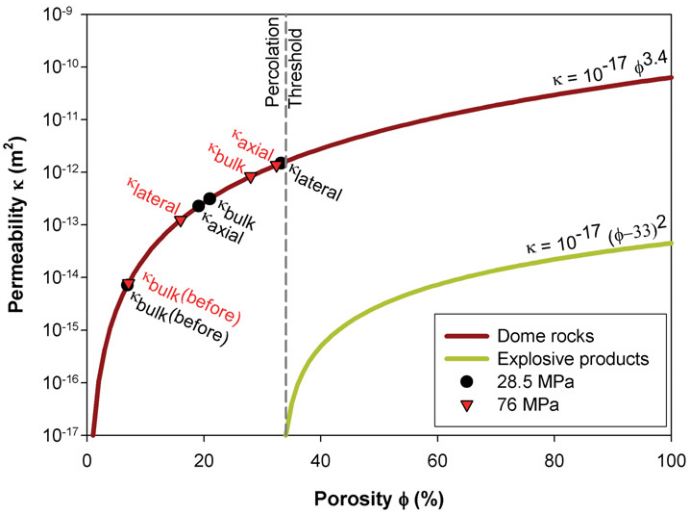

Figure 2. Permeability evolutions during magma failure. The permeabilities "κ_{bulk} (before)" and "κ_{bulk}" were modeled from their relationship with the measured porosity as provided by Mueller et al. (2005). Permeability estimates in the axial (κ_{axial}) and lateral ($\kappa_{lateral}$) directions of the deformed samples were derived through assessment of the crack density obtained by the neutron-computed tomography (NCT) images. The data suggest an increased anisotropy with deformation across the ductile-brittle transition.

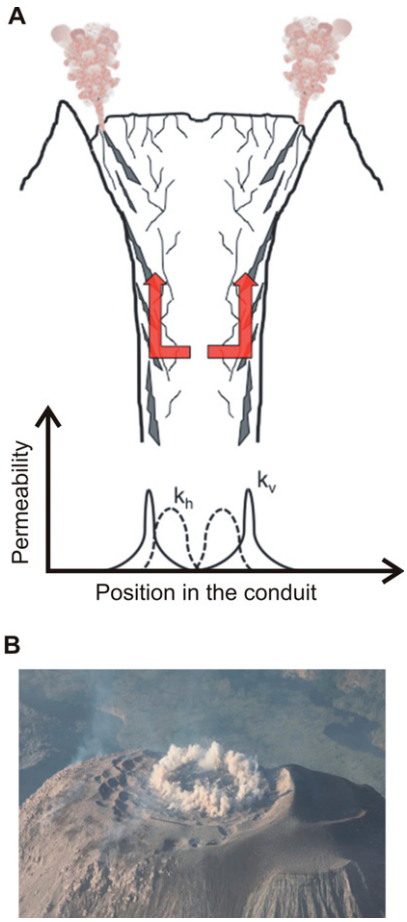

Figure 3. Architecture of permeable fracture network induced by strain localization in magma. A: Localization of strain induces an increase in permeability, promoting outward degassing (red arrows) toward the conduit margins, regions where the magma is subjected to the highest strain rate, causing fractures subparallel to the flow direction, which favor the ascent of gas along larger peripheral fractures. Such anisotropic fracture geometry may explain the formation of gas-and-ash venting along ring structures at Santiaguito volcano, Guatemala (B) (photographer: Richard Roscoe).

for degassing and therefore serves to explain the common occurrence of degassing in the periphery of lava domes (Lavallée et al., 2012; Varley and Taran, 2003) as well as gas-and-ash venting along a ring fracture as seen at Santiaguito volcano (Fig. 3B).

In the implementation of magma rheology to eruptive models, our experimental results suggest that a Maxwell-based approximation of failure cannot explain the strain dependence of crystal-bearing magma rheology. In practice, however, the findings demonstrate that the time window for forecasting magma failure scales with both the progression timescale and imposed stress. This implies that as long as the seismicity originates from magma failure, forecasting may be accurate irrespective of explosive eruption style. Indeed, Vulcanian eruptions at slowly growing and deforming lava domes have been forecast (De la Cruz-Reyna and Reyes-Davila, 2001). More recently, there is growing evidence that rapid fracturing processes during sudden collapse of lava domes may also generate sufficient characteristic seismicity to be used as a forecasting proxy (Hammer and Neuberg, 2009). Regardless of the eruption style, fracturing of magma is required for the occurrence of an explosive eruption, and the development of models to interpret the architecture of magmatic fragmentation via seismicity is therefore an essential component of any accurate hazard mitigation scheme. We conclude that the combination of experimental magma deformation, AE monitoring, and NCT imaging delivers a basis for transferring the conclusions to the field, where deformation and seismic monitoring may ultimately contain the information needed to distinguish not only the timing, but also the style of an impending eruption.

ACKNOWLEDGMENTS

We express our gratitude to J. Neuberg and M. Laumonier for constructive reviews. We acknowledge funding from the DLR, the German Research Foundation (LA2651/1-1, LA2651/3-1, HE4565/2-1), PROCOPE (27061UE), MatWerk, an LMUexcellent Research Professorship, as well as the European Research Council Researcher Grant EVOKES (247076).

REFERENCES CITED

Bai, L.P., Baker, D.R., and Hill, R.J., 2011, Permeability of vesicular Stromboli basaltic glass: Lattice Boltzmann simulations and laboratory measurements: Journal of Geophysical Research (Solid Earth), v. 115, B07201, doi:10.1029/2009JB007047.

De la Cruz-Reyna, S., and Reyes-Davila, G.A., 2001, A model to describe precursory material-failure phenomena: Applications to short-term forecasting at Colima volcano, Mexico: Bulletin of Volcanology, v. 63, p. 297–308, doi:10.1007/s004450100152.

Dingwell, D.B., 1996, Volcanic dilemma: Flow or blow?: Science, v. 273, p. 1054–1055, doi:10.1126/science.273.5278.1054.

Gottsmann, J., Lavallée, Y., Marti, J., and Aguirre-Diaz, G., 2009, Magma-tectonic interaction and the eruption of silicic batholiths: Earth and Planetary Science Letters, v. 284, p. 426–434, doi:10.1016/j.epsl.2009.05.008.

Hale, A.J., and Wadge, G., 2008, The transition from endogenous to exogenous growth of lava domes with the development of shear bands: Journal of Volcanology and Geothermal Research, v. 171, p. 237–257, doi:10.1016/j.jvolgeores.2007.12.016.

Hammer, C., and Neuberg, J.W., 2009, On the dynamical behaviour of low-frequency earthquake swarms prior to a dome collapse of Soufrière Hill volcano, Montserrat: Geophysical Research Letters, v. 36, L06305, doi:10.1029/2008GL036837.

Jellinek, A.M., and Bercovici, D., 2011, Seismic tremors and magma wagging during explosive volcanism: Nature, v. 470, p. 522–525, doi:10.1038/nature09828.

Johnson, J.B., Lees, J.M., Gerst, A., Sahagian, D., and Varley, N., 2008, Long-period earthquakes and co-eruptive dome inflation seen with particle image velocimetry: Nature, v. 456, p. 377–381, doi:10.1038/nature07429.

Kendrick, J.E., Lavallée, Y., Ferk, A., Perugini, D., Leonhardt, R., and Dingwell, D.B., 2012, Extreme frictional processes in the volcanic conduit of Mount St. Helens (USA) during the 2004–2008 eruption: Journal of Structural Geology, v. 38, p. 61–76, doi:10.1016/j.jsg.2011.10.003.

Laumonier, M., Arbaret, L., Burgisser, A., and Champallier, R., 2011, Porosity redistribution enhanced by strain localization in crystal-rich magmas: Geology, v. 39, p. 715–718, doi:10.1130/G31803.1.

Lavallée, Y., Hess, K.U., Cordonnier, B., and Dingwell, D.B., 2007, A non-Newtonian rheological law for highly crystalline dome lavas: Geology, v. 35, p. 843–846, doi:10.1130/G23594A.1.

Lavallée, Y., Meredith, P., Dingwell, D.B., Hess, K.U., Wassermann, J., Cordonnier, B., Gerik, A., and Kruhl, J.H., 2008, Seismogenic lavas and explosive eruption forecasting: Nature, v. 453, p. 507–510, doi:10.1038/nature06980.

Lavallée, Y., Varley, N., Alatorre-Ibargüengoitia, M.A., Hess, K.-U., Kueppers, U., Mueller, S., Richard, D., Scheu, B., Spieler, O., and Dingwell, D.B., 2012, Magmatic architecture of dome-building eruptions at Volcán de Colima, Mexico: Bulletin of Volcanology, v. 74, p. 249–260, doi:10.1007/s00445-011-0518-4.

Main, I.G., Meredith, P.G., and Jones, C., 1989, A reinterpretation of the precursory seismic *b*-value anomaly from fracture mechanics: Geophysical Journal International, v. 96, p. 131–138.

Martel, C., and Schmidt, B.C., 2003, Decompression experiments as an insight into ascent rates of silicic magmas: Contributions to Mineralogy and Petrology, v. 144, p. 397–415, doi:10.1007/s00410-002-0404-3.

Mueller, S., Melnik, O., Spieler, O., Scheu, B., and Dingwell, D.B., 2005, Permeability and degassing of dome lavas undergoing rapid decompression: An experimental determination: Bulletin of Volcanology, v. 67, p. 526–538, doi:10.1007/s00445-004-0392-4.

Neuberg, J.W., Tuffen, H., Collier, L., Green, D., Powell, T., and Dingwell, D., 2006, The trigger mechanism of low-frequency earthquakes on Montserrat: Journal of Volcanology and Geothermal Research, v. 153, p. 37–50, doi:10.1016/j.jvolgeores.2005.08.008.

Noguchi, S., Toramaru, A., and Nakada, S., 2008, Relation between microlite textures and discharge rate during the 1991–1995 eruptions at Unzen, Japan: Journal of Volcanology and Geothermal Research, v. 175, p. 141–155, doi:10.1016/j.jvolgeores.2008.03.025.

Pan, J.-B., Lee, C.-C., Lee, C.-H., Yeh, H.-F., and Lin, H.-I., 2010, Application of fracture network model with crack permeability tensor on flow and transport in fractured rock: Engineering Geology, v. 116, p. 166–177, doi:10.1016/j.enggeo.2010.08.007.

Papale, P., 1999, Strain-induced magma fragmentation in explosive eruptions: Nature, v. 397, p. 425–428, doi:10.1038/17109.

Rutter, E.H., 1986, On the nomenclature of mode of failure transitions in rocks: Tectonophysics, v. 122, p. 381–387, doi:10.1016/0040-1951(86)90153-8.

Scarpa, R., 2001, Volcanology—Predicting volcanic eruptions: Science, v. 293, p. 615–616, doi:10.1126/science.1063606.

Spieler, O., Alidibirov, M., and Dingwell, D.B., 2003, Grain-size characteristics of experimental pyroclasts of 1980 Mount St. Helens cryptodome dacite: Effects of pressure drop and temperature: Bulletin of Volcanology, v. 65, p. 90–104.

Thomas, M.E., and Neuberg, J., 2012, What makes a volcano tick—A first explanation of deep multiple seismic sources in ascending magma: Geology, v. 40, p. 351–354, doi:10.1130/G32868.1.

Tuffen, H., Smith, R., and Sammonds, P.R., 2008, Evidence for seismogenic fracture of silicic magma: Nature, v. 453, p. 511–514, doi:10.1038/nature06989.

Varley, N.R., and Taran, Y., 2003, Degassing processes of Popocatépetl and Volcán de Colima, Mexico, *in* Oppenheimer, C., ed., Volcanic degassing: The Geological Society of London Special Publication 213, p. 263–280.

Voight, B., 1988, A method for prediction of volcanic eruptions: Nature, v. 332, p. 125–130, doi:10.1038/332125a0.

Watts, R.B., Herd, R.A., Sparks, R.S.J., and Young, S.R., 2002, Growth patterns and emplacement of the andesitic lava dome at Soufrière Hills Volcano, Montserrat, *in* Druitt, T.H., and Kokelaar, B.P., eds., Eruption of Soufrière Hills Volcano, Montserrat, from 1995 to 1999: The Geological Society of London Memoir 21, p. 115–152.

Wright, H.M.N., and Weinberg, R.F., 2009, Strain localization in vesicular magma: Implications for rheology and fragmentation: Geology, v. 37, p. 1023–1026, doi:10.1130/G30199A.1.

Manuscript received 13 August 2012
Revised manuscript received 9 November 2012
Manuscript accepted 19 November 2012

Printed in USA